Appl. Phys. B 74, 273–278 (2002)
DOI: 10.1007/s003400200790

Applied Physics B
Lasers and Optics

A. BOSCHETTI[1]
D. BASSI[2]
E. IACOB[2]
S. IANNOTTA[1]
L. RICCI[2]
M. SCOTONI[2,✉]

Resonant photoacoustic simultaneous detection of methane and ethylene by means of a 1.63-μm diode laser

[1] Centro Fisica degli Stati Aggregati, CNR-ITC, 38050 Povo, Trento, Italy
[2] Università di Trento, Dipartimento di Fisica and INFM, 38050 Povo, Trento, Italy

Received: 1 August 2001/Revised version: 28 November 2001
Published online: 7 February 2002 •

ABSTRACT A compact multi-component trace-gas detector based on the resonant photoacoustic technique and a NIR external cavity diode laser has been developed. It has been characterized using a mixture of ethylene and methane diluted in ambient air. A spectroscopic investigation of combination bands and overtones between 5900 and 6250 cm^{-1}, obtained with an IR pulsed laser photoacoustic spectrometer, allowed us to find a wavelength region where the $2\nu_3$ overtone of CH_4 and the $\nu_5 + \nu_9$ combination band of C_2H_4 show uncongested rotational lines. Using a single-mode scan of the diode laser in this region, around 6150 cm^{-1}, the sensitivity for the simultaneous detection of ethylene and methane is 8 ppm/mW and 40 ppm/mW respectively. Factors affecting the sensitivity and selectivity of the detection system and possible improvements suitable to reach the sub-ppm detection limit are discussed.

PACS 42.62.Fi; 42.55.Px; 82.80.Ch

1 Introduction

In recent years, high-sensitivity multi-component gas detectors have found more and more applications in the non-invasive monitoring of many chemical physics processes. Relevant application fields include, for example, combustion processes [1], atmospheric chemistry [2], modified atmospheres for food preservation, ripening and senescence processes in agronomic products [3], plant physiology investigations [4] and medical diagnosis by means of breath analysis [5].

Infrared radiation (IR) spectroscopy can be a valid multi-component detection method, complementary to other well-proven techniques like, for example, mass spectrometry and gas chromatography [6–8]. The major limit of spectroscopic techniques – when applied to 'real' samples – is related to the so-called 'matrix effect', i.e. the interference generated by the possible overlap of absorption bands originating from different molecules that are present in the sample. Thus, both high frequency resolution and wide tunability are necessary to select – for each detected molecule – the best absorption frequency where matrix effects are minimized.

✉ Fax: +39-0461/881-696, E-mail: scotoni@science.unitn.it

At present, near-infrared (NIR) diode lasers are becoming more and more popular due to the recent development of high-quality, compact and cheap sources having a spectral emission which falls in the absorption range of many molecules of great practical interest. The range of the available NIR diode lasers spans from about 0.8 to 2.1 μm. Gas detectors based on fixed-wavelength diode lasers are already commercially available [9] but they are not suitable for the simultaneous detection of more than one molecule. The development of multi-component gas detectors has attracted, in recent years, strong research and technological efforts [10–18]. Detectors based on 1.7–2.1-μm diode lasers are in principle more efficient because many molecules show relatively strong absorption bands in this region, but such lasers are still in development and not easily available. At present, 1.6-μm diode lasers are those that – in the NIR range – provide the best trade-off between cost and molecular detection efficiency. These NIR gas detectors are generally based on the measurement of light attenuation and reach sensitivities in the range of ppb.

In our experiment, we used an alternative approach based on the resonant photoacoustic method. This technique is very well proven and provides huge sensitivities (ppb–ppt range) when used in combination with high-intensity laser sources (power in the range of 100 mW or more), in the frequency range corresponding to fundamental vibrational transitions [19–21]. Photoacoustic detectors are characterized by a very low background signal, and their sensitivity is proportional to the light power. So any power increase due to enhancements of the laser source and/or the use of amplification methods (e.g. intracavity or external build-up cavity configuration) leads to a corresponding increase in the sensitivity.

In this work, we were interested in evaluating the detection limit of resonant photoacoustic methods, when used in combination with a relatively low-power (1 mW) NIR diode laser, operating at 1.63 μm, i.e. coinciding with the first vibrational overtones and combination bands of molecules containing a CH bond. Our prototype system has been optimized for the simultaneous detection of traces of methane (CH_4) and ethylene (C_2H_4) in laboratory air samples. These molecules are important markers for the monitoring of plant physiology and combustion processes.

2 Experimental

The experimental set-up used for this experiment is composed of a commercial NIR diode laser and a resonant photoacoustic cell. The apparatus is shown schematically in Fig. 1.

The laser is an InGaAs diode with broad-band coatings for large tunability mounted in an external cavity in the Littman configuration (Sacher TEC 500). The coarse tuning range is 1590–1670 nm while the fine, single-mode scan is up to 120 GHz with a typical long-term line width of about 2 MHz. The maximum output power is 3 mW.

The single-mode scan is driven by a computer-controlled voltage ramp applied to the grating piezoelectric actuator while it is monitored by a 4-GHz free spectral range air-spaced Fabry–Perot interferometer. Laser intensity and interferometer transmittance are monitored by two GaAs photodiodes and are recorded, together with the photoacoustic signal, for power normalization and wavelength scaling. The laser beam, 2 mm in diameter, can be focused into the cell by means of a 200-mm focal length lens.

The detection system is based on amplitude modulation of laser light in the photoacoustic (PA) cell. This is an open-ended brass tube 100-mm long (L) and 3 mm in radius (R). The frequency of amplitude modulation is chosen so the tube acts as a first acoustic longitudinal mode resonator whose frequency is given by $f_0 = v_s/2L$, where v_s is the velocity of sound. The working frequency is around 1560 Hz and is obtained by modulation of the laser light using a frequency-stabilized ($\Delta f = 1$ Hz) mechanical chopper. The working frequency is optimized by an automatic routine every time gas conditions are changed.

The acoustic cavity opens into decoupling $\lambda/4$ buffer volumes of larger diameter than the resonator. The acoustic signal is detected by a miniature electret microphone (Knowles 1330 EK) coupled to the open resonator at the mid-point where the maximum standing acoustic wave amplitude is located. The quality factor (Q) depends strongly on surface quality of the resonator wall tube as well as upon the coupling between the resonator and microphone volumes. Q values of 50–100 are easily obtainable with careful polishing of the internal surface of the tube and optimum coupling of the microphone cavity. In the present apparatus Q is about 10, providing a very stable and non-critical device, useful for initial evaluation.

The signal generated by photoacoustic absorption is proportional to the pressure wave (Δp) induced by energy transfer from excited molecules to the buffer gas:

$$\Delta p = F(f_0)\alpha W$$

where F is the response function of the cell, α is the gas absorption coefficient and W is the laser power.

F is given by:

$$F(f_0) = (\gamma - 1)LQG/(2\pi f_0 V)$$

where γ is the specific heat ratio of the gas, V is the volume of the cell, G is a geometric parameter and Q is the quality factor of the resonator.

The best performance of the system is obtained by optimization of F, which requires a delicate compromise between the geometrical parameters of the cell and Q, which is proportional to $RL^{-1/2}$ [22]. The signal is amplified by a low-noise preamplifier ($\Delta f \sim 30$ kHz, $\Delta V_{\mathrm{rms}} \sim 4\,\mathrm{nV/Hz^{1/2}}$, gain ~ 2) and then detected by lock-in amplification (EG&G Instruments 7260).

The acoustic resonator is embedded in a massive (about 2 kg) brass body placed on an optical bench in order to minimize sensitivity to external noise sources. The body contains the gas inlet/outlet connections as well as the pre-amplification electronics.

The gas-handling system for purging and filling the cell comprises a vacuum rotary pump and a gas line with pressure and flux control with two inlets for binary mixture preparation inside the cell. The gas system and the cell are connected by a small-diameter (1.5-mm i.d.) teflon tube in order to minimize noise pick-up.

Survey spectra of CH_4 and C_2H_4 have been acquired by means of a pulsed laser system, previously used for molecular beam overtone spectroscopy [23, 24], coupled to a variable-temperature photoacoustic cell developed for pulsed laser spectroscopy [25]. The laser system is a visible dye laser pumped by a Nd-YAG laser (Quantel Datachrome 5000). Infrared radiation between 0.8 and 3.5 μm is obtained by coherent Raman scattering in high-pressure (30 bar) hydrogen. Typical pulse energies and bandwidths are 80 mJ and 3 GHz ($0.1\ \mathrm{cm^{-1}}$) at a 10-Hz repetition rate for dye output and 15, 10 and 2 mJ for the first, second and third Stokes orders respectively. Radiation at 1.6 μm is obtained by the second Stokes shifting of 695-nm dye laser output.

3 Results and discussion

Unambiguous detection and recognition of several components in a gas mixture is possible only if a proper scan

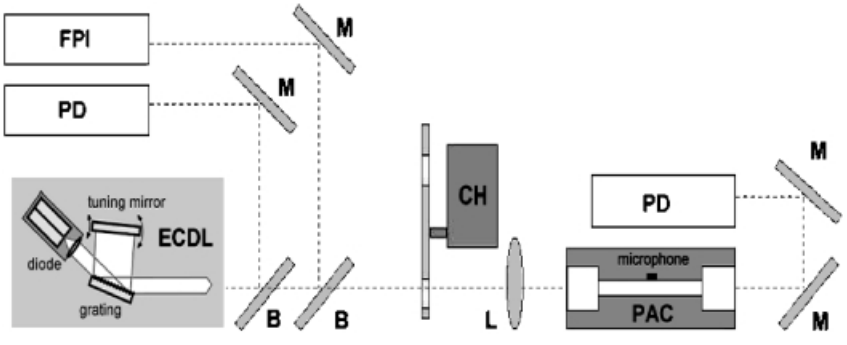

FIGURE 1 Schematic view of the experimental apparatus: ECDL, external cavity diode laser; PAC, resonant photoacoustic cell; FPI, Fabry–Perot interferometer; PD, photodiode; B, beam splitter; M, mirror; L, lens; CH, mechanical chopper. The photodiode placed after the PA cell is for absorption measurements. Overall dimensions are about $25 \times 40 \times 15\ \mathrm{cm^3}$ ($w \times l \times h$)

region is chosen, in which the spectral structures of all systems are clearly identified. In order to simplify the experimental procedure, we limited this detection region to the single-mode scan range of the diode laser (∼ 120 GHz). A wider detection region would require coarse tuning, which would result in mode hopping and cavity misalignment and would consequently require complex and time-consuming procedures to re-calibrate the wavelength and intensity scales, losing the possibility of real-time detection (a few minutes). Because of the relatively small single-mode scan range, preliminary work to identify the best scan region for high-resolution analysis is important. This can be done in principle by analyzing published data and databases. The C_2H_4 IR absorption spectrum between 5850 and 6225 cm^{-1} was measured by Duncan and Ferguson [26] at low resolution: near the $\nu_5 + \nu_9$ band at 6150 cm^{-1} many other overlapped and very congested combination bands are present below 6100 cm^{-1}. Higher-resolution measurement of the $\nu_5 + \nu_9$ band was carried out by Herman and co-workers [27] using a FTIR supersonic slit jet at the Doppler limit. Sub-Doppler investigation by means of molecular beam–optothermal spectroscopy of Q–R branches of the same band was done by Platz and Demtroder [28].

The CH_4 spectral structure in the same region is dominated by the $2\nu_3$ CH stretch band and is available from the HITRAN database.

Our medium-resolution (0.1 cm^{-1}) survey spectra between 5900 and 6250 cm^{-1} of ethylene and methane, obtained with the pulsed laser optoacoustic spectrometer, are shown in Fig. 2a and b respectively and agree well with the published data. In Fig. 2 we also report, as an example, the spectra of some other interesting molecules which might be detected within the tuning range of the diode laser (from the HITRAN 96 database).

The identification of congested spectral structures originated by the overlap of different molecular spectra may be a very difficult task if limited to narrow frequency regions. In order to overcome this problem a wide-range survey spectrum between 5900 and 6250 cm^{-1} of a methane–ethylene mixture was measured. A careful inspection of this measurement was done and some interesting spectral regions were selected for possible mixture identification, around 6026, 6133 and 6156 cm^{-1}. Figure 3b shows a region where a strong (intensity of about 60×10^{-23} $cm^{-1}/(mol\,cm^{-2})$) rotational CH_4 line ($R2$ of $2\nu_3$ band) is distinguishable in a complex and unassigned (near $\nu_5 + \nu_{11}$) C_2H_4 spectral structure with intensities

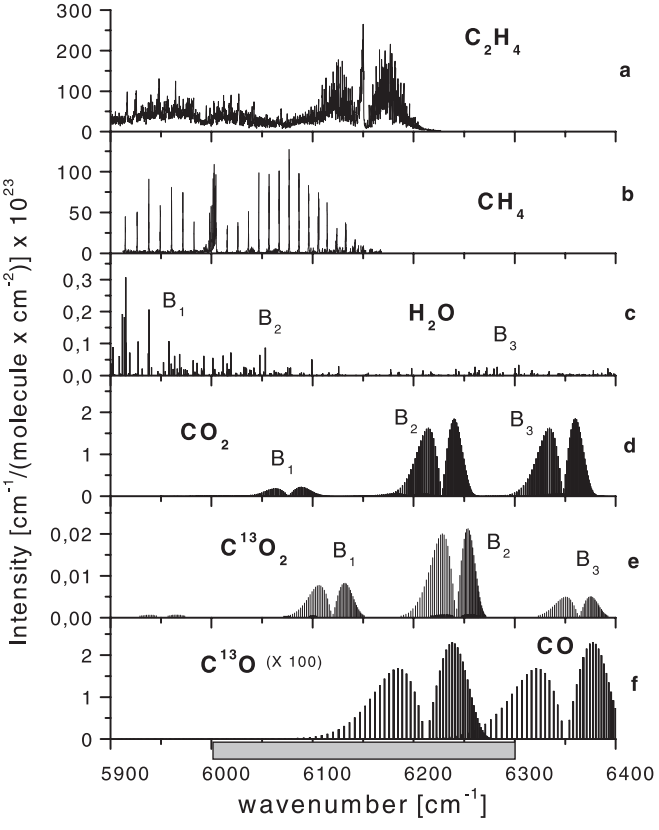

FIGURE 2 Survey spectra between 5900 and 6400 cm^{-1} of C_2H_4, CH_4, H_2O, CO_2 and CO. **a** C_2H_4 spectrum. The PQR rotational structure around 6150 cm^{-1} is assigned to the $\nu_5 + \nu_9$ CH stretch combination band. **b** $2\nu_3$ overtone band of CH_4. **c** H_2O rotational lines of the $\nu_2 + \nu_3$ (B_1), $4\nu_2$ (B_2) and $\nu_1 + 2\nu_2$ (B_3) bands. **d** 30014 ← 00001 (B_1), 30013 ← 00001 (B_2), 30012 ← 0001 (B_3) bands of CO_2. **e** 30013 ← 00001 (B_1), 30012 ← 00001 (B_2), 30011 ← 00001 (B_3) bands of the $C^{13}O_2$ isotope. **f** Third overtone of the most abundant isotopes of CO. Spectra **a** and **b** were obtained by pulsed laser photoacoustic measurement with 10 mbar of C_2H_4 or CH_4 in 50 mbar of Ar at room temperature. Spectra **c**, **d**, **e** and **f** have been obtained from the HITRAN96 database. The wavelength interval shown corresponds to the tuning range of the ECDL (5990–6290 cm^{-1})

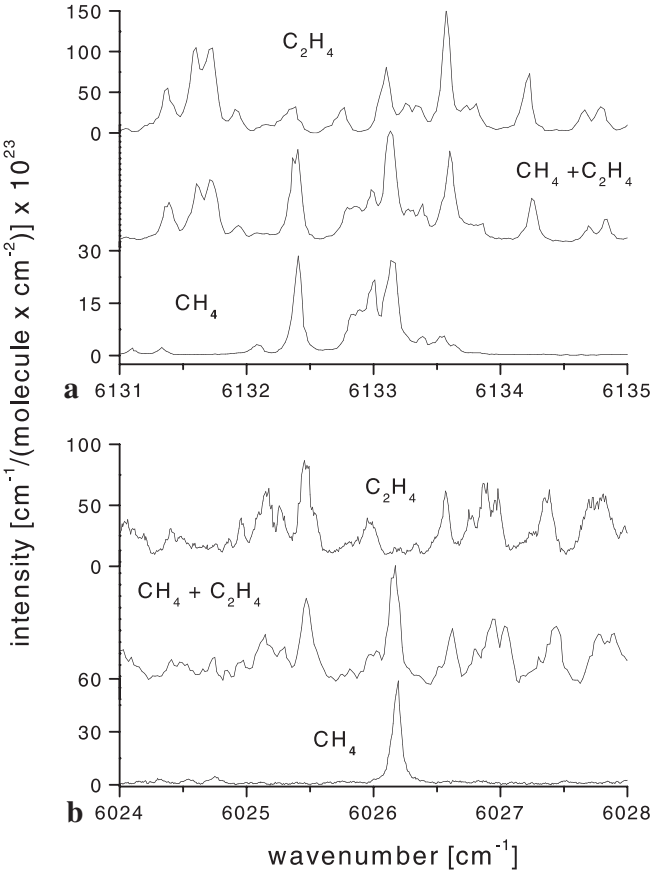

FIGURE 3 Details of survey spectra of an ethylene/methane mixture, together with single-component spectra for comparison, in the regions around 6133 cm^{-1} (**a**) and 6026 cm^{-1} (**b**) carried out with the pulsed laser photoacoustic spectrometer. The total pressure in the PA cell was about 50 mbar: the spectral resolution, about 3 GHz, is due to the laser line width

around 75. Figure 3a shows the rotational structure of the $R13$ transition of methane (with intensity around 30) partially overlapped with strong (intensities of about 120) lines of the P branch of the $\nu_5 + \nu_9$ band of ethylene. In this region, while some prominent lines of C_2H_4 are free of interference from methane, the CH_4 structure is in coincidence with ethylene lines.

Around 6156 cm^{-1}, clearly resolved rotational lines of both systems are present (see Fig. 4). This wavelength region was chosen for the simultaneous detection of ethylene and methane even if the corresponding transition strengths are relatively weak (40 for C_2H_4 and 3.5 for CH_4). Moreover, no relevant interferences from abundant atmospheric components (H_2O, CO_2 and CO) are present in this interval. The CH_4 spectrum shows minor rotational lines, which are reported but not assigned in the HITRAN database. The C_2H_4 rotational transitions were assigned by means of an asymmetric rotor transition calculation program [29], the rotational constants used for the calculation being selected from the literature [27, 28, 30, 31].

In Fig. 5 we show spectra of CH_4, C_2H_4 and a mixture of the two in the same wavelength interval of Fig. 4, obtained with a diode laser 120-GHz single-mode scan. Two clearly separated structures, the ethylene line triplet at 6154.5 cm^{-1} and the methane line triplet at 6157.2 cm^{-1}, are visible while a partially convoluted structure is present between 6156.2 and 6156.7 cm^{-1}.

The spectral resolution necessary for unambiguous identification of the different species can be limited by pressure broadening. For the highest selectivity, low-pressure sampling in the photoacoustic cell is necessary. However the photoacoustic signal intensity depends upon the gas pressure, so in order to obtain the best trade-off between sensitivity and selectivity a suitable working cell pressure has to be found. Pressure dependence of the signal is due to two different factors: (i) the efficiency of the photoacoustic effect reduces when the gas density lowers and (ii) the density of the absorbing species reduces when the mixture is sampled at low

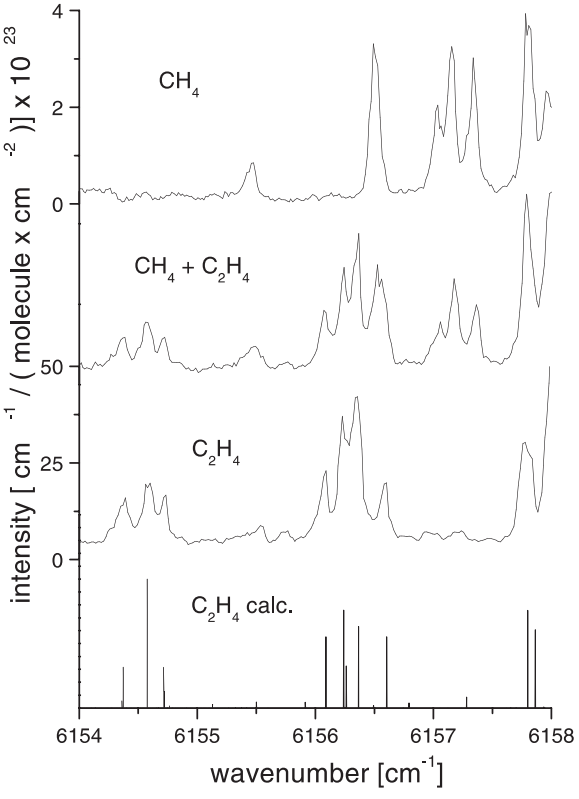

FIGURE 4 Detail of the survey spectrum of the ethylene/methane mixture around 6156 cm^{-1}. This region was chosen for a high-resolution diode laser scan. In the lower trace calculated transitions of the $\nu_5 + \nu_9$ combination band of C_2H_4 are shown. Their assignment $J'(K'_{-1}, K'_{+1}) \leftarrow J(K_{-1}, K_{+1})$ are reported in Table 1

Wavenumber (cm^{-1})	Transitions $J'(K'_{-1}, K'_{+1}) \leftarrow J(K_{-1}, K_{+1})$
6154.36	2 (1 2) ← 1 (1 1)
6154.56	2 (0 2) ← 1 (0 1)
6154.70	2 (1 1) ← 1 (1 0)
6156.07	3 (1 3) ← 2 (1 2)
6156.23	3 (0 3) ← 2 (0 2)
6156.35	3 (2 2) ← 2 (2 1)
6156.59	3 (1 2) ← 2 (1 1)
6157.78	4 (1 4) ← 3 (1 3)
6157.85	4 (3 2) ← 3 (3 1)

TABLE 1 Rotational assignments of the most intense transitions of C_2H_4 between 6154 and 6158 cm^{-1}

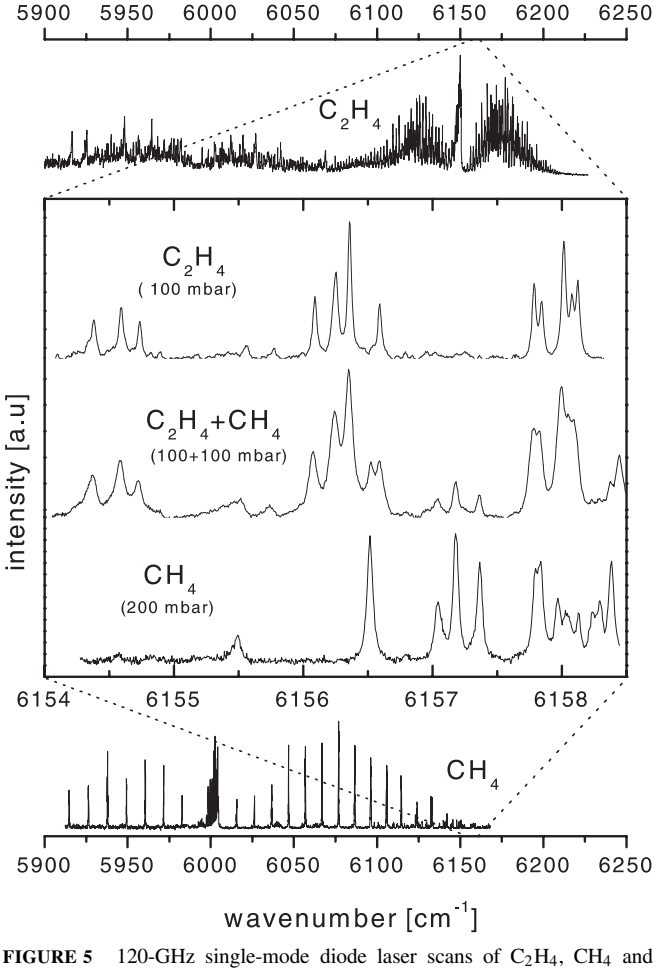

FIGURE 5 120-GHz single-mode diode laser scans of C_2H_4, CH_4 and a 50/50% mixture of the two are shown in the magnified inset. The spectral resolution is determined by pressure broadening

pressure. In order to test the selectivity of the apparatus we restricted our inspection to the partially convoluted structure whose resolution is clearly affected by the pressure broadening. In Fig. 6, 20-GHz scans of a mixture of C_2H_4/CH_4 at different total pressures are shown between 6156.15 and 6156.75 cm^{-1}. The samples are prepared from a mixture containing 5 mbar of both C_2H_4 and CH_4 and adding laboratory air up to the working pressure.

From these measurements it is evident that pressure broadening at atmospheric conditions hides all spectral structure on the scale of tenths of cm^{-1}. Ro-vibrational lines start to be resolved at 300 mbar, where the methane line at 6156.55 cm^{-1} is distinguishable from ethylene lines. The 100-mbar scan shows a clearer pattern where line intensities can be estimated with more accuracy without losing much signal (a factor two in band integral).

A further reduction of the working pressure in the photoacoustic cell produces a strong reduction in the signal, together with the expected resolution enhancement. For example the C_2H_4 doublet at 6156.25 cm^{-1} becomes resolved at 30 mbar, indicating that the working pressure in the cell must be chosen taking into account the density of the combined spectral structures of the molecules to be detected. In the same figure the band integral is reported as a function of total gas pressure as well as the pressure-induced line width: the lower graph clearly show the drop of sensitivity in the photoacoustic effect below 300 mbar while the middle one reports a 5.5 MHz/mbar line broadening and a Doppler limit of about 400 MHz.

In order to estimate the sensitivity of this simple apparatus in the simultaneous detection of CH_4 and C_2H_4 present at equal concentrations, several scans have been performed at different partial pressures and a total gas pressure between 100 and 300 mbar.

In Fig. 7 a spectrum in the same wavelength region as the previous figure, but with ethylene/methane partial pressures of 0.25 mbar in 300 mbar of laboratory air, is shown, corresponding to a concentration of 830 ppm. The line intensity has been measured using the common Leverberg–Marquardt (LM) fitting process with Lorentzian shapes, a procedure which takes only a fraction of a second. The peak positions, widths and relative intensities are fixed, determined by known spectral structures from previous investigations, published data and available databases. The signal-to-noise (S/N) ratio of the C_2H_4 intensity obtained by the analysis of the spectrum shown in Fig. 7 is about 100. This was estimated by comparison with the same fitting procedure performed in a region free of transition lines. The final sensitivity for the detection of C_2H_4 is then about 8 ppm/mW while for CH_4 the limit, in the same frequency region, is about 40 ppm/mW. When the laser power is set at its maximum level, i.e. 3 mW, the sensitivity for C_2H_4 is better than 3 ppm. These values are effective if the C_2H_4/CH_4 concentration ratio does not exceed a factor of 10, otherwise the lower-intensity CH_4 transition is too much embedded in the tails of the stronger C_2H_4 lines.

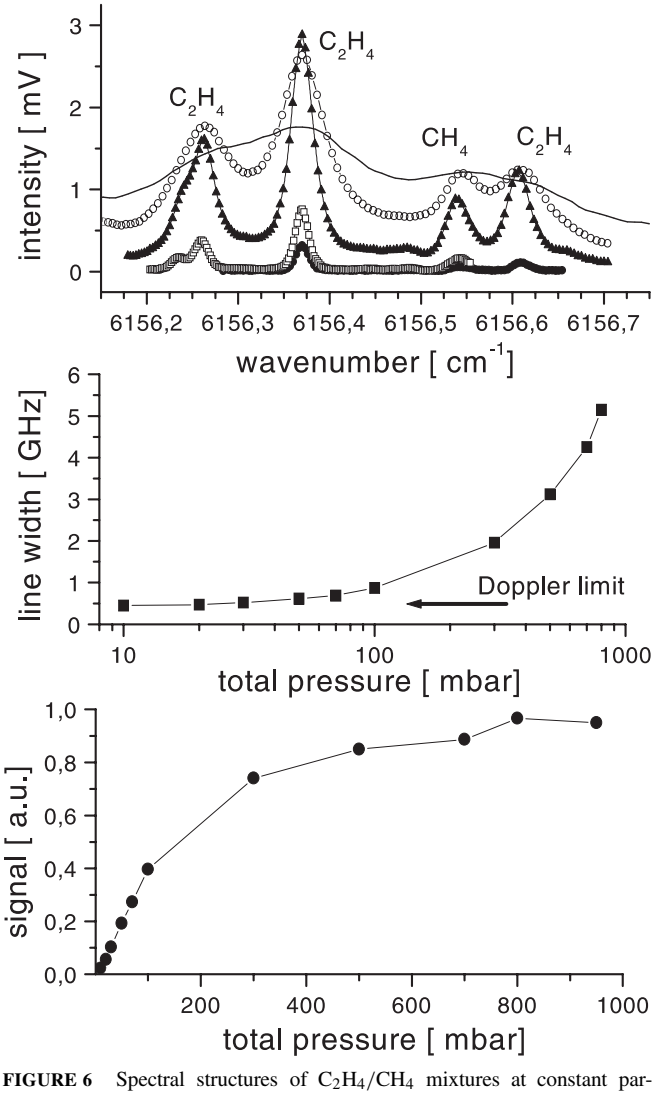

FIGURE 6 Spectral structures of C_2H_4/CH_4 mixtures at constant partial pressures of 5/5 mbar in a cell filled with ambient air at various total pressures (*solid line*, 1000 mbar; *open circles*, 300 mbar; *solid triangles*, 100 mbar; *open squares*, 30 mbar; *solid circles*, 10 mbar). The measured pressure line broadening is reported in the middle graph, while the signal integral as a function of total pressure is shown in the lower one

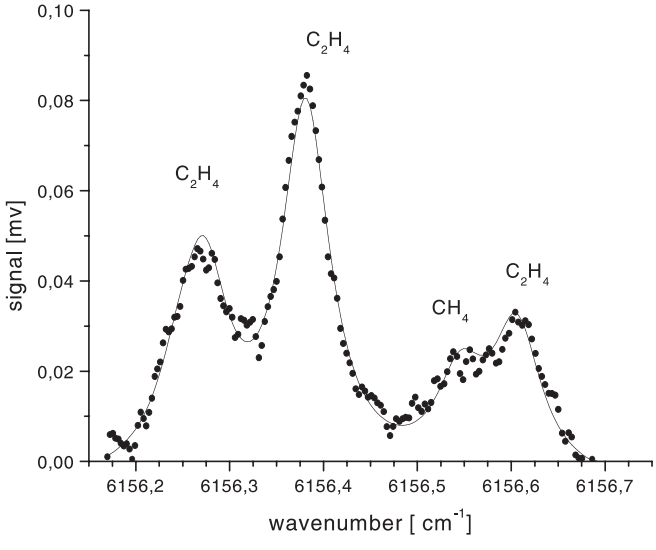

FIGURE 7 Diode laser photoacoustic spectrum of 0.25/0.25-mbar mixture of C_2H_4/CH_4 in 300 mbar of ambient air (*dots*). A multi-peak fit with Lorentzian shapes is shown (*line*)

This problem can be overcome if a wider spectral region is taken into account: the 6154.5 cm^{-1} triplet of ethylene and the 6157.2 cm^{-1} triplet of methane are both inside a single-mode scan and sufficiently wide apart to be detected even if their intensity ratio exceeds 100 (see Fig. 5). At the same time they can be detected unambiguously even at higher pressure, increasing the sensitivity limit with respect to the detection of the congested structure at 6156.4 cm^{-1}. In the case of an atmospheric pressure sample, the 0.25-mbar partial pressure of C_2H_4/CH_4 would correspond to 250-ppm concentration and the same analysis as before leads to a final sensitivity better than 2.5 ppm/mW for C_2H_4 and 12 ppm/mW for CH_4. However the cost to pay is a longer measurimg time. The 20-GHz scan of Fig. 7, obtained with a lock-in time constant of 2 s, takes about 5 min, while a 100-GHz scan requires 25 min in order to reach the same S/N ratio. At present, the sensitivity of the apparatus is essentially limited by external acoustic noise.

4 Conclusions

In this work we have reported the simultaneous detection of ethylene and methane diluted in ambient air, using a single-mode scan of a 1.63-μm laser diode and a resonant PA cell.

The limit sensitivity of the present apparatus for the simultaneous detection is a few ppm/mW for ethylene and tens of ppm/mW for methane. The detection sensitivity, however, strongly depends on required selectivity and concentration ratio of the two species: the right choice of the spectral region together with the best sampling pressure is crucial for obtaining the best performances. As an example an extrapolated sensitivity limit around ppm/mW would be achievable for detecting methane at 6026.25 cm^{-1} or ethylene at 6131.5 cm^{-1} (see Fig. 3).

In order to reach sub-ppm sensitivities with resonant photoacoustic methods and low-intensity lasers, the following aspects should be considered: (a) to increase the radiation intensity inside the cell, (b) to improve the efficiency of the acoustic apparatus and (c) to develop a more efficient signal analysis procedure.

Laser light power enhancement can be achieved (aside with increasing laser performances) by resonant enhancement using a tunable build-up cavity containing the resonant PA cell. The combination of resonant photoacoustics with diode laser radiation enhancement techniques has already been investigated by Bozòki et al. [32]: the PA cell was placed inside the optical cavity of a diode laser, showing a gain in detection efficiency of about 10 with respect to extracavity operation. Placing the resonant PA cell inside an external build-up cavity will provide a higher gain while maintaining the possibility of pressure control in the sampling cell.

The sensitivity of the acoustic apparatus can be increased by improving the mechanical construction and the coupling between the resonant cell and the microphone cavity to reach higher Q factors and external noise rejection.

Furthermore the development of an efficient pattern recognition system will be an important step for S/N enhancement and time saving in the analysis of complex mixtures. The determination of gas concentration in multi-component mixtures by fitting algorithms like LM has already proven to be an effective tool [33]. A promising technique for increasing detection efficiency might come from the recent strong development of neural network technology.

ACKNOWLEDGEMENTS This work has been partially funded by MURST (Sviluppo e Potenziamento dell Attività di Ricerca: Cluster C08-A). The authors wish to thank F. Gottardi and the staff of the mechanics workshop of the Physics Department of the University of Trento for constant help and cooperation. Thanks are also due to Dr. Tim Freegarde who kindly revised the manuscript. It is finally a pleasure to acknowledge Prof. J. Reuss who stimulated the authors to carry out research in this field.

REFERENCES

1 R.M. Mihalcea, D.S. Baer, R.K. Hanson: Appl. Opt. **36**, 8745 (1997)
2 J. Slanina: *Biosphere Atmosphere Exchange of Pollutants and Trace Substances* (Springer, Berlin 1997)
3 J. Oomens, H. Zuckermann, S. Persijn, D.H. Parker, F.J.M. Harren: Appl. Phys. B **67**, 459 (1998)
4 T.W. Kimmerer, T.T. Kozlowski: Plant Physiol. **69**, 840 (1982)
5 S. Koletzko, M. Haisch, I. Seeboth, B. Braden, K. Hengels, B. Koletzko, P. Hering: Lancet **345**, 961 (1995)
6 D. Bassi, P. Tosi, R. Schloegl: J. Vac. Sci. Technol. A **16**, 114 (1998)
7 W. Lindinger, A. Hansel, A. Jordan: Int. J. Mass Spectrom. Ion Process. **173**, 191 (1998)
8 K. Robards, P.R. Haddad, P.E. Jackson: *Principles and Practice of Modern Chromatographic Methods*, 1st edn. (Academic, London 1994)
9 I. Linnerud, P. Kaspersen, T. Jaeger: Appl. Phys. B **67**, 297 (1998)
10 P. Werle, R. Mucke, F. D'Amato, T. Lancia: Appl. Phys. B **67**, 307 (1998)
11 G. Modugno, C. Corsi, M. Gabrysch, F. Marin, M. Inguscio: Appl. Phys. B **67**, 289 (1998)
12 R.M. Mihalcea, M.E. Webber, B.S. Baer, R.K. Hanson, G.S. Feller, W.B. Chapman: Appl. Phys. B **67**, 283 (1998)
13 A. Fried, B. Henry, B. Werth, S. Sewell, J.R. Drummond: Appl. Phys. B **67**, 317 (1998)
14 D.D. Nelson, M.S. Zahniser, J.B. McManus, C.E. Kolb, J.L. Jimenez: Appl. Phys. B **67**, 433 (1998)
15 S. Schafer, M. Mashni, J. Sneider, A. Miklos, P. Hess, H. Pitz, K.U. Pleban, V. Ebert: Appl. Phys. B **66**, 511 (1998)
16 A. Bennen, R. Niesser: Appl. Spectrosc. **53**, 1040 (1999)
17 D.G. Lancaster, D. Richter, F.K. Tittel: Appl. Phys. B **69**, 459 (1999)
18 A. Nadezhdinskii, A. Berezin, S. Chernin, O. Ershow, W. Kutnyak: Spectrochim. Acta A **55**, 2083 (1999)
19 F. Harren, J. Reuss: Encycl. Appl. Phys. **19**, 413 (1997)
20 F. Kuehnemann, K. Schneider, A. Hecker, A.A.E. Martis, W. Urban, S. Schiller, J. Mlynek: Appl. Phys. B **66**, 741 (1998)
21 B. Paldus, T.G. Spence, R.N. Zare, J. Oomens, F.J.M. Harren, D.H. Parker, C. Gmachl, F. Cappasso, D.L. Sivco, J.N. Baillargeon, A.L. Hutchinson, A.Y. Cho: Opt. Lett. **24**, 178 (1999)
22 F.J. Harren: Ph.D. Thesis, University of Nijmegen, The Netherlands (1988)
23 M. Scotoni, M. Zen, D. Bassi, A. Boschetti, M. Ebben: Chem. Phys. Lett. **155**, 233 (1989)
24 D. Bassi, A. Boschetti, M. Scotoni: in *Applied Laser Spectroscopy*, ed. by M. Inguscio, W. Demtroder (Plenum, New York 1990) pp. 215–226
25 D. Bassi, L. Menegotti, S. Oss, M. Scotoni, F. Iachello: Chem. Phys. Lett. **207**, 167 (1993)
26 J.L. Duncan, A.M. Ferguson: J. Chem. Phys. **89**, 4216 (1988)
27 M. Bach, R. Georges, M. Herman, A. Perrin: Mol. Phys. **97**, 265 (1999)
28 T. Platz, W. Demtroder: Chem. Phys. Lett. **294**, 397 (1998)
29 L. Pierce: private communication
30 N. Dam, R. Engeln, J. Reuss, A.S. Pine, A. Fayt: J. Mol. Spectrosc. **139**, 215 (1990)
31 H.C. Allen, E.K. Plyler: J. Chem. Phys. **80**, 2673 (1958)
32 Z. Bozòki, J. Sneider, G. Szabò, A. Miklòs, M. Serényi, G. Nagy, M. Fehér: Appl. Phys. B **63**, 399 (1996)
33 M.A. Moeckli, C. Hilbes, M.W. Sigrist: Appl. Phys. B **67**, 449 (1998)